

Functional subdivisions within anterior cingulate cortex and their relationship to autonomic nervous system function

Scott C. Matthews,* Martin P. Paulus, Alan N. Simmons,
Richard A. Nelesen, and Joel E. Dimsdale

Department of Psychiatry, University of California San Diego, San Diego, CA 92093, USA

Received 30 October 2003; revised 2 March 2004; accepted 3 March 2004

The anterior cingulate cortex (ACC) has diverse functions and several functional subdivisions. This study implemented a counting Stroop task that presented incongruent (INC) and congruent (CON) stimuli at two speeds to probe dorsal (dACC) and ventral (vACC) using functional magnetic resonance imaging (fMRI). Eighteen healthy subjects completed the task twice: once outside the scanner while heart rate variability (HRV) was recorded and once during fMRI. In both sessions, subjects completed two runs. Stimuli were presented every 2.0 s in one run and every 1.5 s in the other. fMRI data analysis revealed two important findings. First, by computing differential activation between INC and CON stimuli, a cluster of activation related to response inhibition was observed in the left dACC. Additionally, by calculating the interaction of speed with stimulus congruency, a cluster of activation was observed in the left vACC. This activation correlated significantly with high-frequency HRV ($P < 0.02$ for CON and $P < 0.003$ for INC) and represents the parasympathetic modulatory role of the vACC. This study supports the notion of functional subdivisions within the ACC and links the processes of cognitive interference and parasympathetic modulation with activation in specific subregions of the ACC, a structure that is critical for the interface between cognition and emotion.

© 2004 Elsevier Inc. All rights reserved.

Keywords: Anterior cingulate cortex; Incongruent stimuli; Congruent stimuli; fMRI; Heart rate variability

Introduction

The anterior cingulate cortex (ACC) is a structure in the medial prefrontal cortex (PFC) with diverse functions. Functional subdivisions have been previously outlined, which distinguish between the cognitive and affective regions within this structure (Bush et al., 1998; Vogt et al., 1992; Whalen et al., 1998). In particular, the cognitive (dorsal) division of the ACC is important for mediating processes such as response inhibition (Bush et al., 1998) and error processing (Carter et al., 1998). In comparison, the affective

(ventral) subdivision is involved in the processing and integration of emotional information (Mayberg, 1997; Simpson et al., 2001).

The neural pathways involved in these processes are closely related to those involved in modulation of the autonomic nervous system (ANS). For example, stimulation of the human rostral cingulate elicits bradycardia and an increase in blood pressure (Pool and Ransohoff, 1949). Cardiovascular responses have also been observed with stimulation of the human orbitofrontal and insular cortices (Oppenheimer et al., 1992), areas that are anatomically and functionally connected to the ACC. Additionally, recent functional magnetic resonance imaging (fMRI) work has demonstrated the importance of the ACC in modulating sympathetic nervous system (SNS) tone (Critchley et al., 2003).

Heart rate variability (HRV) may be viewed as an experimental measure of cardiovascular adaptability. Large variability in heart rate is associated with physical fitness and youth. Conversely, physical and mental illnesses, as well as physical and psychological stressors, are associated with decreased HRV. The sympathetic and parasympathetic subdivisions of the ANS each play a role in regulating heart rate and other homeostatic processes. Postganglionic parasympathetic nervous system (PNS) fibers release acetylcholine (ACh), a neurotransmitter with a rapid onset and course of action. As a result, beat-to-beat (high-frequency) changes in heart rate are mediated by the PNS and reflected in high-frequency HRV. Conversely, SNS neurons release norepinephrine (NE), which is characterized by a slower on/offset. Therefore, SNS influences on heart rate are largely reflected in very low frequency HRV.

The Stroop Word–Color interference task (Stroop, 1935) has been used in psychophysiological studies to probe HRV (Delaney and Brodie, 2000; Hoshikawa and Yamamoto, 1997). Additionally, the neural substrates underlying the cognitive processes involved in the Stroop are well characterized and involve the response inhibitory function of the ACC. The current study examined the hypothesis that ANS modulation by the ACC is intimately related to the cognitive processing functions of this structure. To examine this hypothesis, healthy control subjects twice performed a Stroop task: once during functional magnetic resonance imaging (fMRI) and again outside the MRI scanner while HRV was recorded. Because the Stroop task elicits HRV changes in behavioral paradigms (Delaney and Brodie, 2000; Hoshikawa and Yamamoto, 1997) and because the ACC has been implicated both in inhibitory function and top-down control of

* Corresponding author. San Diego Veterans Administration Health Services, 3350 La Jolla Village Drive, Mail Code 116A, La Jolla, CA 92161. Fax: +1-858-642-6442.

E-mail address: scmatthews@ucsd.edu (S.C. Matthews).

Available online on ScienceDirect (www.sciencedirect.com.)

the ANS, we hypothesized that this task would lead to alterations in ANS functioning and brain activation in the ACC. Moreover, we hypothesized that task-induced ANS changes would correlate with task-induced changes in brain activation in the ACC. In the following sections, we will describe the results of this experiment and suggest future research directions that may contribute to the understanding of the link between ACC function and ANS modulation.

Methods

Subjects

Eighteen (7 females and 11 males) healthy subjects gave written informed consent and completed the study. The mean age of participants was 39 years (range 27–56), and the average education level of the population was 14.9 years (range 12–18). All subjects completed the structured clinical interview for *DSM IV* and had no lifetime history of any Axis I *DSM IV* disorder. The UCSD Human Research Protection Program approved this study.

Task

The current study implemented a counting Stroop task (Bush et al., 1998; Stroop, 1935), with stimuli containing between one and three rows of numbers. The numbers in each row are either “1,” “2,” or “3.” Subjects were instructed to press the mouse button corresponding to the number of rows presented on the screen.

Our task implements congruent and incongruent stimuli (Fig. 1). For congruent stimuli, the meaning of the numbers in each row and the number of times the number appears in each row facilitate the correct response (the number of rows). Conversely, for incongruent stimuli, subjects must inhibit both the meaning of the numbers in each row and the amount of numbers in each row to correctly identify the number of rows.

To determine whether processing speed contributed to the cognitive interference component of the task, two task runs were completed during each of two study sessions. Subjects performed one “fast” run and one “slow” run (described below), while HRV data were collected and on a different day during fMRI. All runs lasted 8 min 32 s and began with 8 s of blank screen, followed by 24 s of a fixation cross, then nine stimulus blocks (five congruent blocks and four incongruent blocks presented in an alternating fashion). This was followed by another 24-s fixation block, then by

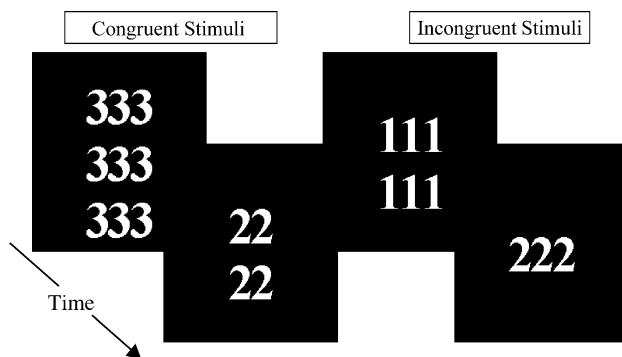


Fig. 1. Counting Stroop stimuli. Digits in each row are either “1,” “2,” or “3.” Subjects are instructed to press the mouse button that corresponds to the number of rows presented on the screen.

nine stimulus blocks (four congruent and five incongruent blocks presented in alternating fashion), and finally another 24 s of fixation cross. Each stimulus block consisted 18 s of stimulus presentation followed by 6 s of blank screen.

“Fast” runs correspond to 1500-ms trials and consisted eighteen 24-s stimulus blocks (nine congruent and nine incongruent). For each trial, the stimulus was presented for 1000 ms followed by a 500-ms blank-screen interstimulus interval. “Slow” runs contained 2000-ms trials (a 1500-ms stimulus presentation followed by a 500-ms blank-screen interstimulus interval) and also consisted 18 stimulus blocks (9 congruent and 9 incongruent).

All subjects performed two runs (one slow and one fast) inside the scanner and two identical runs during HRV testing. For all testing sessions, the slow run was performed before the fast run.

Behavioral measures

For all subjects, mean error rate and reaction time were calculated for all runs. All analyses for the behavioral data were carried out with SPSS 10.0 (Norusis, 1990). A mixed-model ANOVA (fixed factor: task conditions; random factor: subjects) was used to analyze the behavioral measures. Comparisons were evaluated using the least significant difference post hoc analysis. Subjects were excluded if their mean reaction time or mean error rate was more than three standard deviations from the group mean.

Physiologic monitoring

Heart rate data were acquired using an I-330 C-2 portable 6-channel physiological monitoring and biofeedback hardware system, and Physiolab software (hardware and software made by J and J Engineering Poulsbo, WA). Physiological data were collected for each subject by placing a ground lead on the left index finger and one EKG lead on each wrist. Artifact was removed by editing out data points (beats) that deviated by more than three standard deviations from the beats that immediately preceded or followed the discrepant beat. Data were then interpolated from the surrounding beats. Subjects were excluded if 5% or more of beats were edited. The Heart Rate Variation Analysis program (Version beta 1.3, Baylor College of Medicine 1996) implemented a fast Fourier transformation on R–R interval data to obtain power values for high (0.4–0.15 Hz), low (0.15–0.04 Hz), and very low (<0.04 Hz) frequency spectra. These ranges were based on previously established standards defined in the special report on HRV by the Task Force of the European Society of Cardiology and the North American Society of Pacing and Electrophysiology (1996). While the 24-s trial lengths did not permit measurement of HRV changes associated with specific incongruent and congruent trials, peak power values were extracted from the high and very low frequency spectra over the entire fast and slow runs and correlated with percent signal change values in the dorsal and vACC. Because both sympathetic and parasympathetic influences are reflected in the low-frequency (0.15–0.04 Hz) range of HRV, correlations were not examined between peak power values in the low frequency range and brain activation.

Functional magnetic resonance imaging

Each scanning session lasted approximately 1 h and was performed using a 1.5-T Siemens Vision Scanner at the University of California San Diego (UCSD). Sessions consisted a three-plane

scout scan (10 s), a high-resolution anatomic scan covering the whole brain, a series of T2*-weighted echoplanar imaging (EPI) scans to measure blood oxygen level-dependent (BOLD) functional activity, and an EPI-based field map to correct for susceptibility-induced geometric distortions. Imaging experiments were performed on a 1.5-Tesla Siemens (Erlangen, Germany) scanner (T2*-weighted echoplanar imaging, repetition time = 2000 ms, echo time = 40 ms, 64 × 64 matrix, twenty 4-mm axial slices). Each run was acquired in sessions of 256 repetitions and lasted 8 min and 32 s. During the same experimental session, a T1-weighted image (MPRAGE, TR = 11.4 ms, TE = 4.4 ms, flip angle = 10°, FOV = 256 × 256, 1-mm³ voxels) was obtained for anatomical reference.

All structural and functional image processing and analysis were performed with the Analysis of Functional Neuroimages (AFNI) software package (Cox, 1996). To minimize motion artifact, echoplanar images were realigned to the 128th acquired scan. Additionally, data were time-corrected for slice acquisition order. Time series data for each individual were analyzed using a multiple regression model. Two regression analyses were carried out, one for the fast run and one for the slow run. For each regression, seven regressors were entered into this model including two task conditions (i.e., congruent and incongruent), three motion parameters (i.e., yaw, pitch, and roll), one linear drift regressor, and the baseline condition (fixation cross). Before inclusion in the regression model, the task-related regressors were convolved with a gamma variate function (Boynton et al., 1996) to account for the hemodynamic delay and the slow rise and fall of the hemodynamic response. The resulting beta weight for the congruent and incongruent condition was divided by the baseline regressor to obtain percent signal difference. A 6-mm full-width half-maximum Gaussian filter was applied to the voxelwise percent signal difference data to account for individual variations in anatomical landmarks. Each subject's data were normalized to Talairach coordinates (Talairach and Tournoux, 1988), and a whole-brain mask was applied to screen out nonbrain voxels and voxels falling within the artifact region.

The voxelwise percent signal difference data for both runs for all subjects were entered into a mixed-model three-way ANOVA with speed ("fast" or "slow") and condition (congruent or incongruent) as fixed factors and subjects as a random factor. To determine areas that significantly activated with cognitive challenge, data from the fast and slow runs were combined and a within-subjects contrast was computed between the incongruent and congruent stimuli irrespective of task speed. A threshold-cluster method was then applied. This threshold adjustment method was based on Monte Carlo simulations and was used to guard against identifying false-positive areas of activation (Forman et al., 1995). Based on these simulations, it was determined that a voxelwise a priori probability of 0.05 would result in a corrected clusterwise activation probability of 0.05 if a minimum volume of 500 μ l and a connectivity radius of 4.0 mm were considered. Finally, the average percent signal difference for each subject during each task condition was extracted from regions of activation, which were found to survive this threshold/cluster method. In a *s* analysis, the interaction of task speed with stimulus congruency was examined. The same threshold-cluster method was applied, and regions of interest were extracted from areas that survived this analysis.

Relational analysis

Percent signal differences obtained from functional regions of interest, which were obtained via the cluster-threshold/volume

method described above, were correlated with peak power values within the high and very low frequency domains of HRV. All correlational analyses were carried out with SPSS.

Results

Behavioral

Behavioral results are displayed in Table 1. Individual performance was comparable during fMRI and HRV testing sessions. Specifically, during HRV testing, subjects made more errors [$F(1, 13) = 131, P < 0.001$] and took longer to respond [$F(1, 13) = 306, P < 0.001$] in the incongruent relative to the congruent trials. Similarly, during fMRI testing, subjects made more errors [$F(1, 13) = 86, P < 0.001$] and took longer to respond [$F(1, 13) = 335, P < 0.001$] in the incongruent relative to congruent trials. Because error rate was low during all testing conditions, significant correlations were not observed between error rates during fMRI and HRV sessions. However, response latency was highly correlated across the two testing sessions (Table 1). Thus, performance was highly comparable and reliable during the fMRI and HRV testing sessions.

Autonomic nervous system

Four subjects were excluded from the autonomic analysis for the following reasons: (1) the mean response latency for one subject was more than three standard deviations from the group mean, (2) one subject was taking a β -adrenergic blocking medication that affects ANS tone, and (3) two subjects' heart rate data contained more than 5% artifact. For the remaining 14 subjects, fluctuations in high and very low frequency bands of HRV over the course of the task were analyzed.

Brain activation

Congruency effect

The congruency effect was calculated by subtracting activation related to congruent stimuli (irrespective of task speed) from activation related to incongruent stimuli (irrespective of task speed). For the congruency effect, large clusters of activation were observed in the left superior parietal lobule and right precuneus, as well as the bilateral insula and dorsal ACC (dACC).

Table 1
Error rate and response latency related to a counting Stroop task during brain imaging and autonomic testing

Trials	% Errors		Response latency		
	Autonomic ^a	Imaging ^a	Autonomic ^a	Imaging ^a	<i>r</i>
1.5-s Trials					
Incongruent	4.4 (2.4)	5.4 (2.3)	622 (56)	646 (46)	0.739**
Congruent	0.9 (1.8)	0.8 (1.3)	521 (49)	539 (43)	0.673*
2.0-s Trials					
Incongruent	2.8 (1.8)	3.5 (2.0)	704 (65)	756 (54)	0.820**
Congruent	0.9 (1.0)	1.2 (1.0)	581 (66)	623 (63)	0.735**

^a Mean (SD).

* $P < 0.005$.

** $P < 0.001$.

Table 2
Brain activation related to a counting Stroop task

Area (Brodmann area)	Side	Volume	x	y	z
<i>Interaction effect^a</i>					
Inferior parietal lobule (40)	right	960	54	-43	29
Inferior parietal lobule (40)	left	832	-45	-40	52
Middle frontal gyrus (6)	left	768	0	1	58
Middle temporal gyrus (37)	right	704	49	-54	0
Middle frontal gyrus (6)	left	704	-25	-8	57
Ventral anterior cingulate (24)	left	640	-9	26	0
Ventral anterior cingulate (32)	left	640	-12	37	8
Posterior cingulate (23)	left	512	-5	-52	14
Inferior occipital gyrus (19)	left	512	-41	-79	-4
<i>Congruency effect^b</i>					
Superior parietal lobule (7)	left	24,064	-30	-58	43
Precuneus (7)	right	13,824	26	-60	42
Insula + inferior frontal gyrus (9)	left	10,688	-39	13	21
Insula (13)	right	10,496	39	16	18
dACC + medial frontal gyrus (6)	left	9408	-17	-6	58

^a All clusters contain at least eight contiguous voxels, each significant at $P < 0.05$. For the interaction effect, all clusters meeting the above criteria and $>500 \text{ ml}^3$ are reported.

^b All clusters contain at least eight contiguous voxels, each significant at $P < 0.05$. For the interaction effect, all clusters meeting the above criteria and $>9000 \text{ ml}^3$ are reported.

Interaction (congruency vs. trial duration) effect

The speed by congruency effect was determined by calculating differential activation related to congruent and incongruent stimuli for fast and slow speeds. Areas of activation for the congruency and speed by congruency analyses are listed in Table 2. For the interaction effect, activation in bilateral inferior parietal lobule, left middle frontal gyrus, right medial temporal lobe, and ventral ACC (vACC) was observed. Consistent with our initial hypotheses, the following two activation patterns are particularly noteworthy:

1. A significant cluster of activation was observed in the left dACC related to the effect of stimulus congruency (Fig. 2).

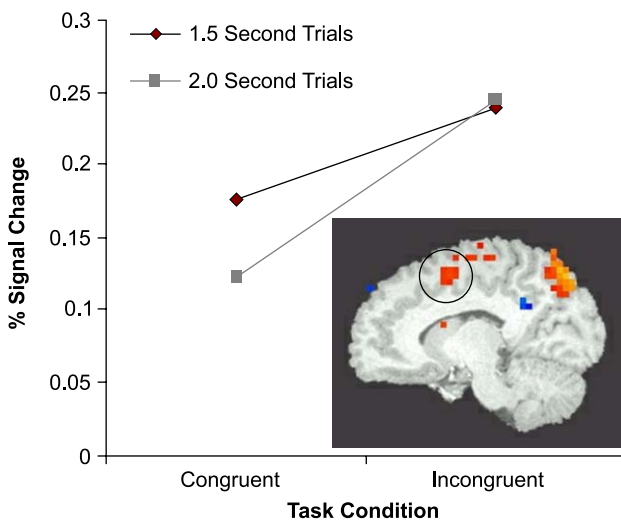


Fig. 2. Dorsal anterior cingulate activation related to Stroop task main effect of stimulus congruency. All clusters contain at least eight contiguous voxels, each significant at $P < 0.05$.

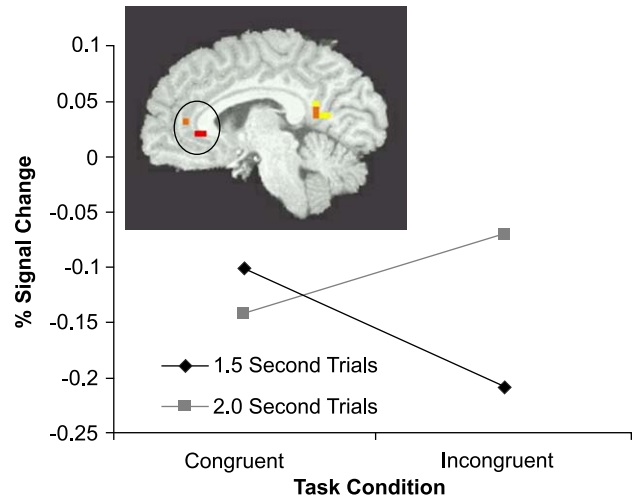


Fig. 3. Ventral anterior cingulate activation related to Stroop task interaction effect of stimulus congruency with task speed. All clusters contain at least eight contiguous voxels each significant at $P < 0.05$.

2. A significant cluster of activation was observed in the left vACC related to the interaction of task speed with stimulus congruency (Fig. 3).

Because our initial hypotheses related to the effect of the Stroop task on ACC function and ANS activity, we performed correlational analysis between these parameters (reported below).

Relational findings

Several correlational analyses were conducted. Specifically, task-related percent signal change values from the dACC and vACC were correlated with peak power values from the high and very low spectra of HRV (Table 3). No significant correlations were observed between dACC activation and HRV peak power

Table 3
Relationships between brain activation and heart rate variability during a counting Stroop task

Area of activation	Condition	Heart rate variability			
		High frequency		Very low frequency	
		r	P	r	P
Ventral ACC					
	Slow				
	Congruent	0.386	0.173	0.544	0.044
	Incongruent	0.259	0.371	0.485	0.079
	Fast				
	Congruent	0.612	0.020	-0.437	0.118
	Incongruent	0.724	0.003	-0.120	0.682
Dorsal ACC					
	Slow				
	Congruent	-0.419	0.136	0.102	0.728
	Incongruent	-0.308	0.285	-0.060	0.839
	Fast				
	Congruent	-0.322	0.262	0.019	0.948
	Incongruent	0.010	0.972	-0.007	0.981

values. However, the following significant correlations were observed:

1. Peak high-frequency HRV over the entire fast run significantly correlated with activation in left vACC during congruent trials ($r = 0.612$, $P = 0.02$).
2. Peak high-frequency HRV over the entire fast run significantly correlated with activation in left vACC during incongruent trials ($r = 0.724$, $P = 0.003$).

Discussion

This study yielded three main results:

1. Subjects performed the Stroop task similarly during HRV and fMRI testing.
2. Increased task-related ACC activation was observed. As expected, the dACC was activated during the incongruent relative to the congruent condition. Additionally, significant activation of the vACC was observed, which was related to the interaction of task speed by stimulus congruency.
3. Within individual subjects, the degree of activation in the vACC, but not the dorsal ACC, correlated significantly with the peak high-frequency HRV.

Taken together, these results provide support for the hypothesis that ANS modulation by the ACC is closely related to the cognitive processing function of this structure. Prior studies have described dACC activation related to cognitive interference tasks (Bush et al., 1998) and emphasized the role of this structure in mediating cognitive processes such as error processing and response inhibition. Similarly, we report increased dACC activation related to response inhibition, a finding that adds to an established body of literature supporting the role of the dACC in processing cognitive information.

Various other functions have also been ascribed to the vACC. Specifically, the vACC and its anatomical connections, such as the anterior insula and medial temporal lobe structures such as the amygdala, play a role in modulation of the ANS. In fact, recent studies have described the importance of the ACC, both dACC and vACC, in modulating the SNS (Critchley et al., 2003). In the current study, the observed relationship between high-frequency HRV and activation in the vACC provides evidence of the role of the vACC in modulation of the PNS.

The ANS is critical for maintenance of homeostasis and proper functioning of all organ systems in the body. Normal bodily processes such as respiration may affect ANS tone. Additionally, factors such as physical illness and psychological stress (Delaney and Brodie, 2000; Hoshikawa and Yamamoto, 1997) may also perturb the ANS. HRV is a noninvasive technique that allows for a reliable and accurate measure of the SNS and PNS components of ANS tone. Time domain measures of HRV provide gross estimates of overall autonomic state. More complex spectral analyses that describe HRV frequencies explain the relative contributions of the PNS and SNS to overall autonomic tone. Changes in high-frequency HRV reflect parasympathetic tone, whereas SNS activity is reflected, although not exclusively, in very low frequency HRV (Pumprla et al., 2002).

The delicate balance between SNS and PNS activity is regulated by brain stem and diencephalic structures such as the hypothalamus,

medulla, and pons. Additionally, there are “higher” cortical structures such as the ACC, insula, and medial temporal lobe structures such as the amygdala and hippocampus, which are connected with lower centers. As a whole, these cortical structures have been called the central autonomic network (CAN) (Benarroch, 1993) and function to integrate emotional and cognitive information and exert a modulatory role on lower brain centers that control the ANS.

fMRI and other neuroimaging techniques have greatly advanced our understanding of the relationship between the human CAN and cardiovascular system. Recent studies have described that states of peripheral arousal are represented within the central nervous system (Damasio, 1999) and that specific structures, including the pons and insula, are critically involved in the representation of states of peripheral arousal (Critchley et al., 2001). Related studies have outlined the role that the ACC plays in the modulation of the SNS (Critchley et al., 2003). In summary, various evidence supports the concept of an integrated CAN, including cortical centers as well as brain stem and diencephalic structures, which is involved in the representation of states of peripheral autonomic arousal as well as the modulation of the ANS. The current study provides evidence of PNS modulation by the vACC and is consistent with this evidence.

There were limitations in this study. While we did not simultaneously acquire HRV and BOLD signal, strong correlations between behavioral data inside and outside of the magnet implied that a common process was engaged during physiological monitoring and fMRI and that the observed correlations between vACC activation and high-frequency HRV were legitimate. In the future, it will be important to acquire HRV and BOLD signal data simultaneously to better understand their relationship. Additionally, due to short trial lengths in this block design, it was not possible to obtain measures of HRV spectral components during individual trials or to determine correlations between HRV and brain activation over specific trials. Other studies have measured simultaneously HRV and brain activation using event-related fMRI, providing the opportunity to measure HRV and brain activation changes related to individual stimuli. Similarly, in the current study, spectral components of HRV were not orthogonalized with one another and, while the low-frequency range of HRV was not used in correlational analyses, we cannot definitively state that the observed high-frequency power values were representative of “pure” PNS tone. Additionally, while we did observe group-averaged dACC activation, we did not observe dACC activation in all subjects. Finally, we cannot rule out the fact that a practice effect may have played a role in this study, as the slow run was administered before the fast run to all subjects both inside the scanner and during HRV testing.

Despite these limitations, this study provides important data that support the concept of functional subdivisions within the ACC, including the PNS modulatory function of the vACC. The counting Stroop was useful in probing two specific subdivisions. Specifically, by observing the effect of stimulus congruency, the role of the dACC in mediating response inhibition was evidenced. Furthermore, by analyzing the interaction of task speed with stimulus congruency, vACC activation was observed, which was related to PNS tone. This complements an established body of literature by Critchley et al. describing the role of the dACC in ANS modulation. While the ACC does contain functionally and anatomically distinct subregions, various evidence has emerged which implicates both the dACC and vACC in ANS modulation. Tasks that induce robust activation within specific functional subdivisions within the ACC, in individual subjects, have been

developed (Bush et al., 2003) and should be used in future experiments. In conclusion, this study provides evidence that ACC functioning during a cognitive challenge task is closely linked to modulation of HRV. Therefore, ACC functioning is not limited to conflict or error detection, but it also relates to the top-down control of the internal milieu via modulation of the ANS.

References

- Benarroch, E.E., 1993. The central autonomic network—Functional organization, dysfunction, and perspective. *Mayo Clin. Proc.* 68 (10), 988–1001.
- Boynton, G.M., Engel, S.A., Glover, G.H., Heeger, D.J., 1996. Linear systems analysis of functional magnetic resonance imaging in human V1. *J. Neurosci.* 16 (13), 4207–4221.
- Bush, G., Whalen, P.J., Rosen, B.R., Jenike, M.A., McInerney, S.C., Rauch, S.L., 1998. The counting Stroop: an interference task specialized for functional neuroimaging-validation study with functional MRI. *Hum. Brain Mapp.* 6 (4), 270–282.
- Bush, G., Shin, L.M., Holmes, J., Rosen, B.R., Vogt, B.A., 2003. The multi-source interference task: validation study with fMRI in individual subjects. *Mol. Psychiatry* 8 (1), 60–70.
- Carter, C.S., Braver, T.S., Barch, D.M., Botvinick, M.M., Noll, D., Cohen, J.D., 1998. Anterior cingulate cortex, error detection, and the online monitoring of performance. *Science* 280 (5364), 747–749.
- Cox, R.W., 1996. AFNI: software for analysis and visualization of functional magnetic resonance neuroimages. *Comput. Biomed. Res.* 29 (3), 162–173.
- Critchley, H.D., Mathias, C.J., Dolan, R.J., 2001. Neuroanatomical basis for first- and second-order representations of bodily states. *Nat. Neurosci.* 4 (2), 207–212.
- Critchley, H.D., Mathias, C.J., Josephs, O., O’Doherty, J., Zanini, S., Dewar, B.K., et al., 2003. Human cingulate cortex and autonomic control: converging neuroimaging and clinical evidence. *Brain* 126 (Pt. 10), 2139–2152.
- Damasio, A.R., 1999. *The Feeling of What Happens: Body and Emotion in the Making of Consciousness*. Harcourt Brace, New York.
- Delaney, J.P.A., Brodie, D.A., 2000. Effects of short-term psychological stress on the time and frequency domains of heart-rate variability. *Percept. Mot. Skills* 91 (2), 515–524.
- Forman, S.D., Cohen, J.D., Fitzgerald, M., Eddy, W.F., Mintun, M.A., Noll, D.C., 1995. Improved assessment of significant activation in functional magnetic resonance imaging (fMRI): use of a cluster-size threshold. *Magn. Reson. Med.* 33 (5), 636–647.
- Hoshikawa, Y., Yamamoto, Y., 1997. Effects of Stroop color-word conflict test on the autonomic nervous system responses. *Am. J. Physiol.* 272 (3 Pt. 2), H1113–H1121.
- Mayberg, H.S., 1997. Limbic-cortical dysregulation: a proposed model of depression. *J. Neuropsychiatry Clin. Neurosci.* 9 (3), 471–481.
- Norusis, M.J., 1990. *SPSS Base System User’s Guide*. SPSS Inc., Chicago.
- Oppenheimer, S.M., Gelb, A., Girvin, J.P., Hachinski, V.C., 1992. Cardiovascular effects of human insular cortex stimulation. *Neurology* 42 (9), 1727–1732.
- Pool, J.L., Ransohoff, J., 1949. Autonomic effects on stimulating the rostral portion of the cingulate gyri in man. *J. Neurophysiol.* 12, 385–392.
- Pumprla, J., Howorka, K., Groves, D., Chester, M., Nolan, J., 2002. Functional assessment of heart rate variability: physiological basis and practical applications. *Int. J. Cardiol.* 84 (1), 1–14.
- Simpson Jr., J.R., Drevets, W.C., Snyder, A.Z., Gusnard, D.A., Raichle, M.E., 2001. Emotion-induced changes in human medial prefrontal cortex: II. During anticipatory anxiety. *Proc. Natl. Acad. Sci. U. S. A.* 98 (2), 688–693.
- Stroop, J.R., 1935. Studies of interference in serial verbal reactions. *J. Exp. Psychol.* 18, 643–662.
- Talairach, J., Tournoux, P., 1988. *Co-planar Stereotaxic Atlas of the Human Brain: A 3-Dimensional Proportional System, An Approach to Cerebral Imaging*. Thieme Medical Publishers, New York.
- Task Force of the European Society of Cardiology and the North American Society of Pacing and Electrophysiology, 1996. Heart rate variability: standards of measurement, physiological interpretation and clinical use. *Circulation* 93 (5), 1043–1065.
- Vogt, B.A., Finch, D.M., Olson, C.R., 1992. Functional heterogeneity in cingulate cortex: the anterior executive and posterior evaluative regions. *Cereb. Cortex* 2 (6), 435–443.
- Whalen, P.J., Bush, G., McNally, R.J., Wilhelm, S., McInerney, S.C., Jenike, M.A., et al., 1998. The emotional counting Stroop paradigm: a functional magnetic resonance imaging probe of the anterior cingulate affective division. *Biol. Psychiatry* 44 (12), 1219–1228.